Zeitschrift: Helvetica Physica Acta
Band: 42 (1969)
Heft: 5

Artikel: Investigation on colour centres in alcaline earth fluorides
Autor: Bill, H.
DOI: https://doi.org/10.5169/seals-114094

Investigation on Colour Centres in Alcaline Earth Fluorides

by **H. Bill**
Institut de Physique Expérimentale, Université de Genève

(20. III. 69)

Abstract. Two new colour centres in alcaline earth fluorides are investigated in this article. Both are due to the impurities oxygen and yttrium and they are only observed with EPR after the crystals have been X rayed. In fact the X rays change the valence state of the impurity complexes formed during growth or by hydrolysing the appropriately doped crystals thus creating the paramagnetic centres. One of them consists of a (YO_2) molecule substitutionally located in the crystal. The other centre involves one O^- ion in substitutional position nearby a Y^{3+} ion. Their model and the informations about their electronic structure have been deduced from EPR, ENDOR, optical measurements, annealing experiments and in the case of the (YO_2) also by investigating the centre produced with water enriched in ^{17}O. The results are described by the appropriate spin Hamiltonians. The centre (YO_2) is shown to form approximately a $(Y^{3+} - O_2^{3-})$ structure. The other centre has its magnetic electron located predominantly in a p_z orbital of the O^- ion involved. The thermal annealing experiments performed on samples containing both centres and Y^{3+} ions exhibit after appropriate treatment of the samples charge transfert from the less stable centre involving one O^-ion to the $(YO_2)^-$ molecule ion (transfert of holes). The annealing experiments further show that the optical transition observed at 486 mμ in CaF_2 and at 510 mμ in SrF_2 arises from the (YO_2) centre.

Résumé. Dans ce travail deux centres colorés trouvés dans des fluorures alcalinoterreux sont étudiés. Ils sont dus à la présence simultanée d'yttrium et d'oxygène dans ces cristaux et ils sont formés en irradiant les échantillons aux rayons X. En effet, les rayons X produisent les centres en changeant la valence des complexes d'impuretés constitués lors de la formation du cristal (ou en hydrolysant des cristaux dopés à l'yttrium). Tous les deux centres sont paramagnétiques. L'un d'eux consiste en une molécule (YO_2) et l'autre se compose essentiellement d'un ion O^- situé au voisinage directe d'un ion Y^{3+}.

Leur modèle et les informations concernant leur structure électronique ont été déduits des mesures RPE, ENDOR et optiques et des expériences de recuit. En plus le centre (YO_2) a été produit en utilisant de l'eau enrichie en ^{17}O et la *shf* de cet isotope a été mesurée. Les expériences de résonance sont décrites par des Hamiltoniens de spin adéquats. Il résulte de ces investigations que le centre (YO_2) est approximativement de la structure $(Y^{3+} - O_2^{3-})$ et que l'électron magnétique de l'autre centre est surtout localisé dans une orbitale p_z de l'ion O^-. On démontre par des expériences de recuit que de la charge peut être transférée d'une espèce de centres à l'autre (transfert de trous) dans des cristaux contenant les deux espèces et de l'yttrium Y^{3+} en même temps. En plus ces expériences permettent de prouver que la transition optique observée à 486 mμ dans CaF_2 et à 510 mμ dans SrF_2 est probablement due au centre (YO_2).

Introduction

It is well-known that many species of colour centres can easily be produced in commercially available synthetic alcaline earth fluoride crystals or in natural fluorites. Most of them involve impurities.

Trivalent rare earth ions (REions) are easily incorporated substitutionally into the fluorite structure. Due to the empty cubes present in this lattice the compensation of the excess positive charge is accomplished by supplementary fluoride ions lo-

cated on such sites. The fluoride ions are situated either adjacent to the impurity producing an axial crystal field at the REion or they are located at some distance from the REion the latter then being in an approximately cubic environment.

The anions can easily be substituted by oxygen ions which diffuse at high temperatures into the crystal (BONTINCK [1], SIERRO [2]).

The investigations underlying this article have shown that the oxygen plays an important part in the formation of many of the colour centres, and that the fundamental mechanism of hole trapping discovered by KÄNZIG [3, 4] is involved for their ionisation. The oxygen ions diffuse during hydrolysis of the crystal (or in the melt when oxygen is added there) to the trivalent cationic impurities present. X raying of the treated crystals at ambient temperatures yields a kind of molecule ions each involving the oxygen which has trapped a hole and the neighbouring cationic impurity for certains of the trivalent impurities. In very pure samples the oxygen ions form under X irradiation a molecular bond with the anions (BILL, LACROIX [5]). Centres of both kinds have been observed in CaF_2, SrF_2 and BaF_2 and partly also in $SrCl_2$ and SrClF.

In this article are analyzed examples of the kind of impurity centres described. They involve beside the oxygen the element yttrium contained in the host lattices CaF_2 and SrF_2. One of the centres reported consists essentially of a O^- ion situated in direct neighbourhood of a Y^{3+} ion. The other centre is a (YO_2) molecule. Both centres have trapped a hole and both are paramagnetic. Their structure is deduced from the results obtained from Electron Paramagnetic Resonance (EPR), Electron Nuclear Double Resonance (ENDOR) optical and annealing experiments, as is reported in the following sections.

Along the investigations underlying this article we have profited considerably from the large store of knowledge about colour centres in alcali halides. Detailed references are for instance found in the book of SCHULMAN and COMPTON [6]. Furthermore the article of O'CONNOR and CHEN [7] has been very helpful at the beginning of the investigations.

Experimental Procedures

Sample Preparation

All the crystals used in this investigation have been produced in our laboratory using the Bridgeman-Stockbarger technique. The crystals were grown in high vacuum ($\leqslant 10^{-5}$ mmHg) or in an atmosphere of purified argon. Ultrapure carbon crucibles were used. The starting materials were purchased from British Drug House, England ('OPTRAN' quality) and from Merck, Germany ('ULTRAPUR' quality).

We introduced the desired cation impurity into the crystals by adding the corresponding metal fluoride to the melt. The distribution coefficient of yttrium between the melt and the solid phase is very near to unity in CaF_2 and SrF_2 (O'CONNOR and CHEN [7]). Thus homogeneously doped crystals can be grown.

The concentration of the introduced impurities was measured by means of X ray fluorescence. With the same technique the amount of unwanted impurities was determined.

The oxygen was introduced into the crystals by heating them in sealed quartz tubes (evacuated before by a water jet pump) to about 900 °C for some hours, or by

heating them in a quartz tube connected at one end to a water jet pump and at the other to a small bottle containing some water (SIERRO [2]). Another method consisted by adding to the melt a given amount of alcaline earth oxyde. In this case the crystals were grown in vitreous carbon crucibles manufactured by 'Le Carbone, France'. This method produces fully transparent crystals even with a relatively high oxygen concentration ($\leqslant 0.15\%$).

The ratio of the concentration of oxygen and yttrium involved during growing and heat treatment of the crystals determines whether one or the other (or both) of the investigated centres are found in the resulting samples after X raying. At high oxygen level the (YO_2) centre is preferentially found whereas at low oxygen concentration the centre involving one oxygen ion is produced.

The oxygen content of the samples was determined by EPR. In fact, the presence and the intensity of the two oxygen centres described in this article give the desired information.

For our experiments with ^{17}O we used water containing 14.2% of this isotope [8]. The ^{17}O was introduced into the crystals by hydrolysis. Several pure and yttrium doped crystals were annealed in an rf heated platinum crucible inside a sealed pyrex envelope containing the ^{17}O water. The water vapor pressure was determined by the temperature of the glass wall and amounted typically to about 1/5 to 1/2 atmosphere.

We oriented all our samples by using the (1, 1, 1) cleavage planes or by Laue diffraction patterns.

Apparatus

The crystals (approximately $2\times4\times8$ mm) were exposed at room temperature for several hours to the infiltered radiation of a X ray tube with tungsten target and beryllium windows. The tube was operated at 45 kV peak Voltage and about 20 mA. The dose rate at the crystal location was about 200 r/h. In order to approach a homogeneous coloration the samples were irradiated usually from all sides. The EPR experiments were performed on a Varian X band spectrometer with superheterodyne adapter. The optical absorption was measured with a Beckman DK2a. The ENDOR equipment has been used for the detailed investigation of the surroundings of the (YO_2) centre. A representative signal to noise ratio observed of those measurements is about 50:1 (1 sec). The frequency of the lines is determined with $\pm$ 8 kHz accuracy from marks at every MHz recorded with the spectrum. The bleaching experiments realized at temperatures higher than the room temperature were performed in an oil bath where the crystal was held for 6 minutes at the desired temperature.

Models of the Centres and Qualitative Description of Their EPR Spectra

The Centre $(YO_2)^0$

The Model

Figure 1 shows the model of the $(YO_2)^0$ centre as it resulted from the analysis of the spectra. It consists of a Y^{3+} substituting for a calcium ion and two neighbouring O^{2-} ions located on fluorine sites. The complex has trapped a hole during X raying of the crystal and thus can be considered as a neutral (YO_2) molecule. It is paramagnetic with spin 1/2.

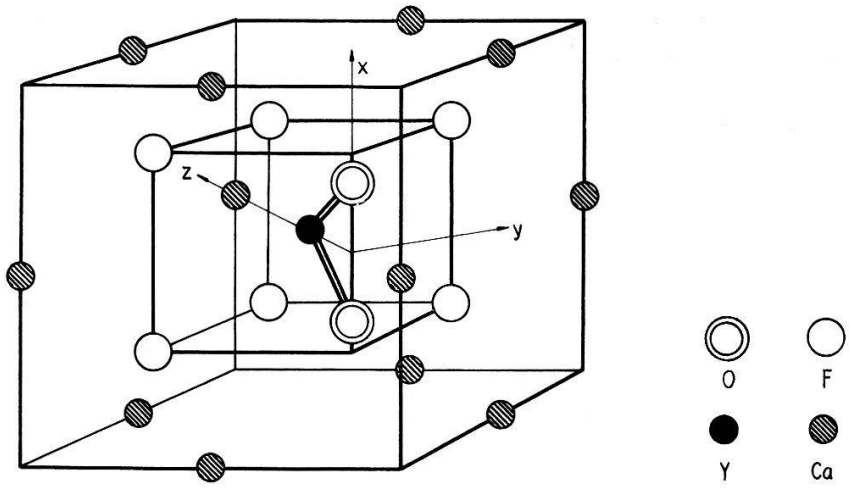

Figure 1

Model of the (YO_2) centre imbedded into the fluorite structure. Its principal axes are x, y, z. The direction of $\vec{B}$ is specified by the angles ϑ, φ. The polar angle ϑ is given with respect to z, the azimuthal angle φ lying in the (x, y) plane is measured with respect to x.

Note that the structure of Y_2O_3 is similar to the CaF_2 structure. The yttrium ions occupy the positions corresponding to the calcium sites and the oxygen is located at the fluoride sites. However, since oxygen is bivalent, only 3/4 of the fluoride sites are occupied by them. The resulting structure is the one of Tl_2O_3 (WYCKOFF [9]). The (YO_2) molecule can thus be considered as a building block of such a crystal.

Qualitative Analysis of the EPR Spectra

The symmetry of the centre is orthorhombic (C_{2V}). Its principal axes x, y, z are indicated in Figure 1. The symmetry implies that there are 12 equivalent possible orientations. Of these only 6 are distinguishable by magnetic resonance (as long as no electric field is applied to the crystal). In the Figures 2a, b and 3a, b are reproduced

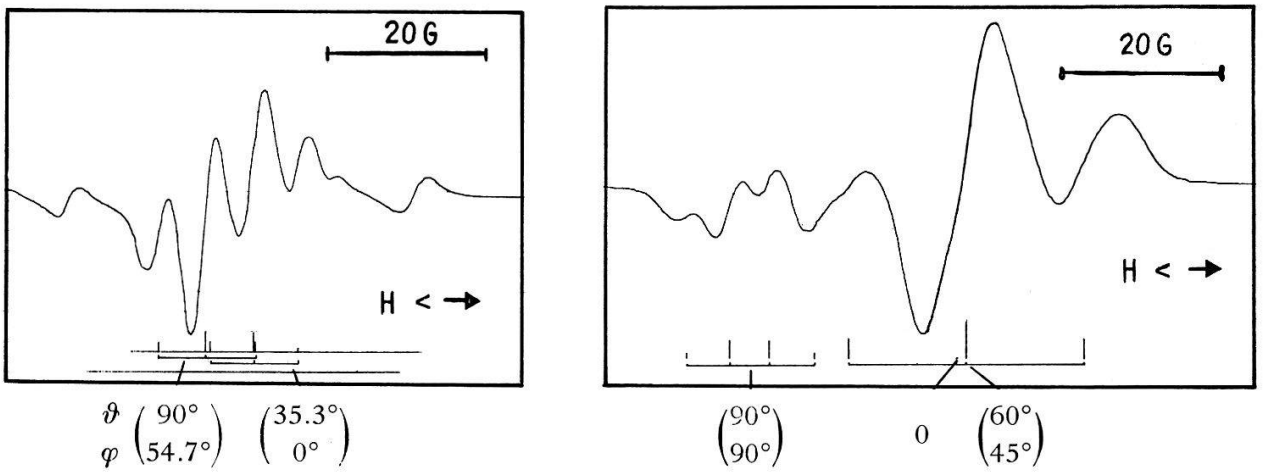

Figures 2a, b

Spectra of the (YO_2) centre in CaF_2 ($T = 20\,°C$); see figure 1 for the definition of ϑ, φ.

Fig. 2a: $\vec{B} \parallel [1, 1, 1]$. The triplets arise from the F^- shfs interaction (nuclei 4, 5 in figure 10).

Fig. 2b: $\vec{B} \parallel [1, 1, 0]$ the spectrum $\vartheta = 90°$ shows the resolved shfs interaction with the two F^- nuclei and the hfs with the yttrium (nucleus 1 in figure 10).

the EPR spectra for some special directions of $\vec{B}$. The different equivalent orientations of $\vec{B}$ are labeled with respect to *one* centre instead of giving the different equivalent centres with respect to the given direction of $\vec{B}$.

The EPR spectra exhibit resolved hyperfine interaction of the electronic spin with the yttrium nucleus ($I = 1/2$) and the two neighbouring fluorine nuclei ($I = 1/2$) on the x axis (nuclei 4 and 5 in Figure 10).

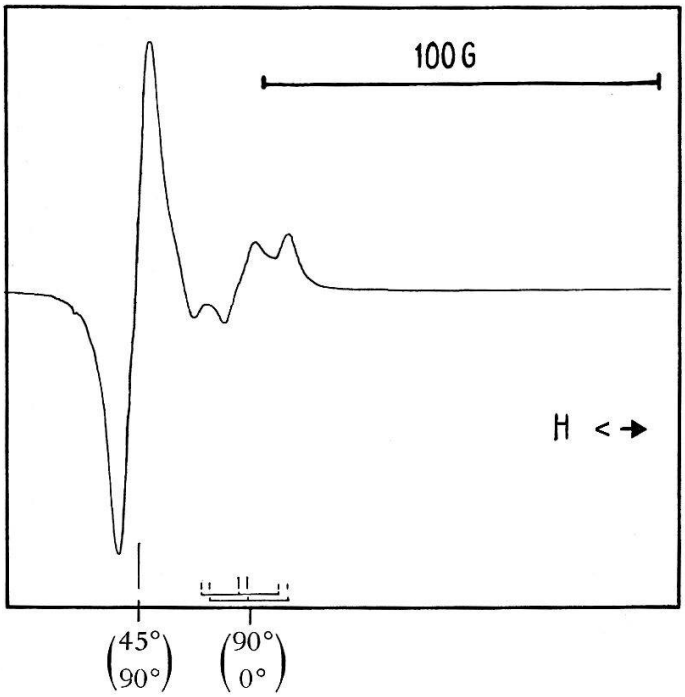

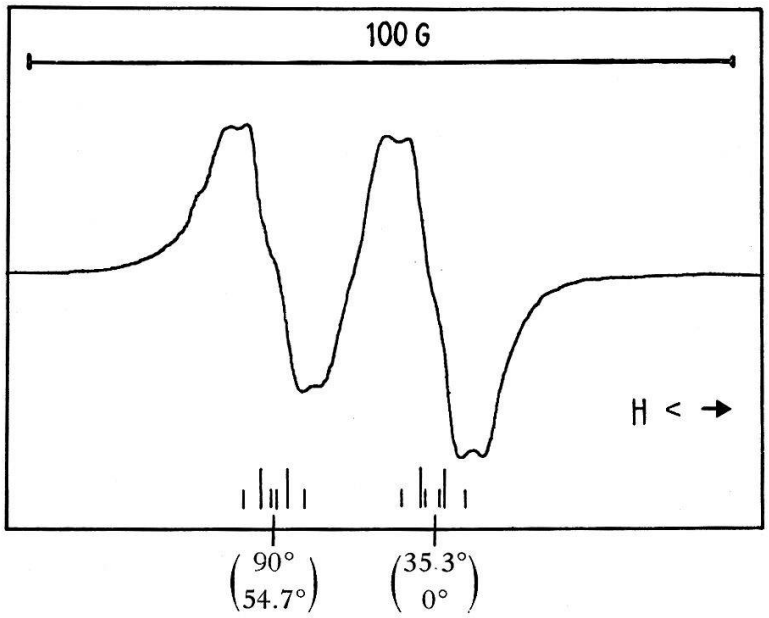

Figures 3 a, b

Spectra of the (YO_2) centre in SrF_2 ($T = 20\,°C$). See Figure 1 for the definition of ϑ, φ. The splitting of the different lines is due to the shfs interaction of the two equivalent F^- ions (nuclei 4, 5 in Figure 10) and due to the yttrium ion implied in the centre.

Fig. 3 a: $\vec{B} \parallel [0, 0, 1]$. Fig. 3 b: $\vec{B} \parallel [1, 1, 1]$.

The deviation from axial symmetry of the fluorine hf interaction as well as the deviation from spherical symmetry of the one of the yttrium are so small that they do not show in ordinary EPR spectra.

Therefore it is not possible to make the assignment of g_{yy} and g_{zz} to the corresponding experimentally determined values unless one uses the isotope ^{17}O.

After X raying crystals doped with ^{17}O enriched water one observes besides $(Y^{16}O_2)$ the $(Y^{16}O^{17}O)$. The centre $(Y^{17}O_2)$ has not been observed.

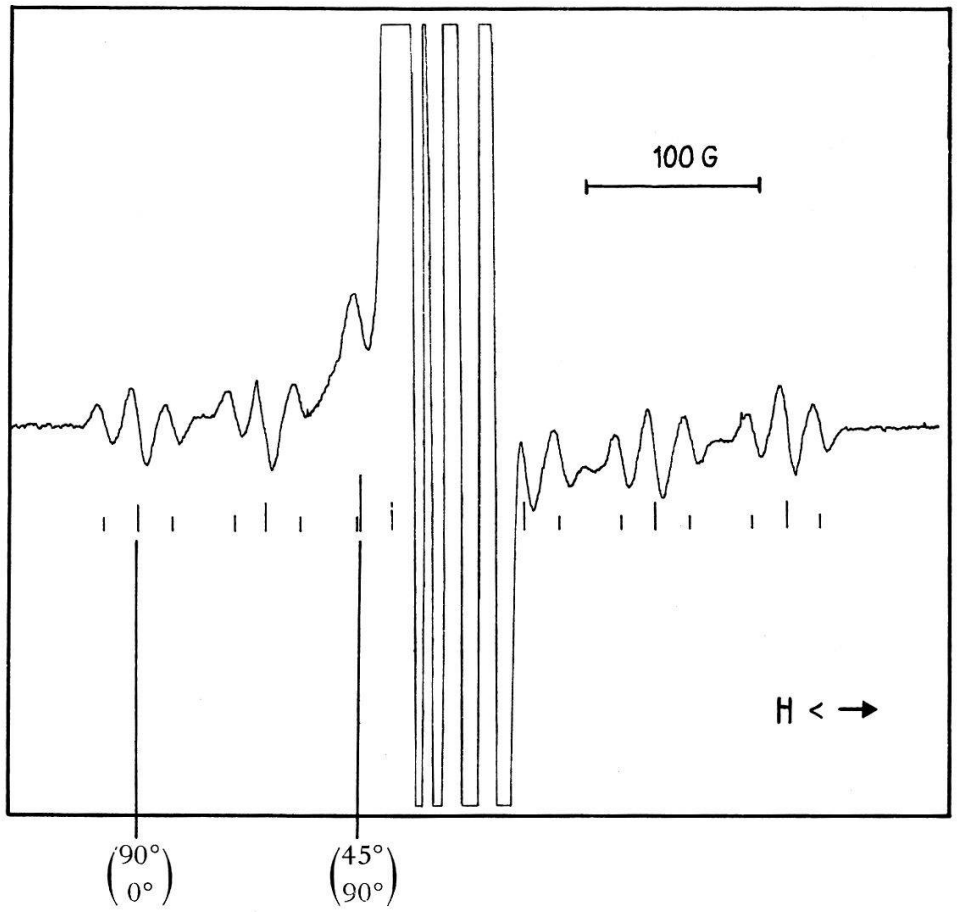

Figure 4

Spectrum of the $(Y^{16}O^{17}O)$ centre in CaF_2. $\vec{B} \parallel [0, 0, 1]$. The strong lines arise from the $(Y^{16}O_2)$ and the remainder from the $(Y^{16}O^{17}O)$. The six triplets (one is hidden by the $(Y^{16}O_2)$ spectrum) labelled $\vartheta = 90°$, $\varphi = 0°$ correspond to $\vec{B} \parallel x$ in figure 1. The splitting between the triplets is due to the ^{17}O hfs, and the triplet splitting arises from the F^- neighbours (nuclei 4, 5 in Figure 10). At the low field side of the $(Y^{16}O_2)$ spectrum one line of the $\vartheta = 45°$, $\varphi = 90°$ spectrum of $(Y^{16}O^{17}O)$ is visible.

The EPR spectra of the centre $(Y^{16}O^{17}O)$ show the sextett splitting due to the nuclear spin 5/2 of the isotope ^{17}O (see the Figures 4 and 5 a, b). The ^{17}O hfs permits to fix the orientation of the molecular plane with respect to the measured g values (with the exception of g_{xx}, which is assigned already from the spectra of $(Y^{16}O_2)$). Symmetry arguments require that one of the principal axes (η_1, η_2, η_3 of Figure 11) of the ^{17}O hfs is directed perpendicular to the molecular plane. The two others are lying in it and are tilted by an (experimentally determined) angle δ_0 with respect to

the x and z axes. A detailed but quite standard further analysis shows that the axis perpendicular to the plane is easiest identified from the spectrum taken with $\vec{B} \parallel [1, 1, 1]$.

The experimental spectra for CaF_2 and SrF_2 (Figure 5a) yield that g_{yy} corresponds to the one of the two measured but unassigned components of g whose numerical value is greatest.

The ^{17}O hfs enables a determination of the number of oxygen ions implied in the centre. The line intensity ratio of the centres ($Y^{16}O_2$) and ($Y^{16}O^{17}O$) has been determined from the spectrum with $\vec{B} \parallel [0, 0, 1]$ (Figure 4) and compared to a theoretical value calculated from the known concentration of the isotope ^{17}O in the enriched water (taking into account the dilution during doping). The obtained figures show very good agreement for *two* oxygen ions being implied, thus confirming the model (YO_2).

The Centre Involving One Oxygen Ion

The model of this centre is not unambiguously established. Its EPR spectra involve an orthorhombic g tensor and two almost axially symmetric hfs interactions. One is roughly directed along a fourfold and the other along a threefold crystal axis.

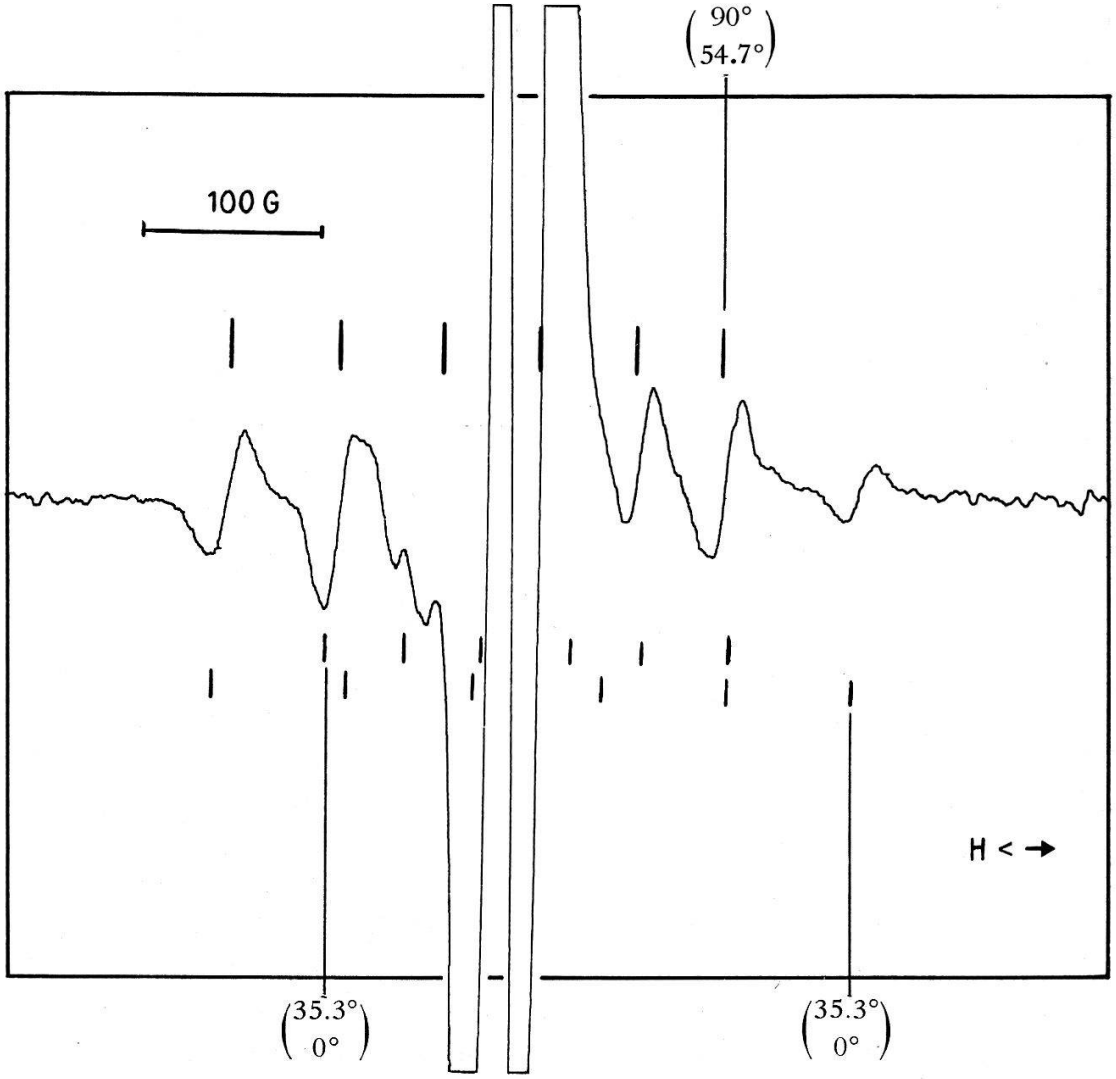

Figure 5 a

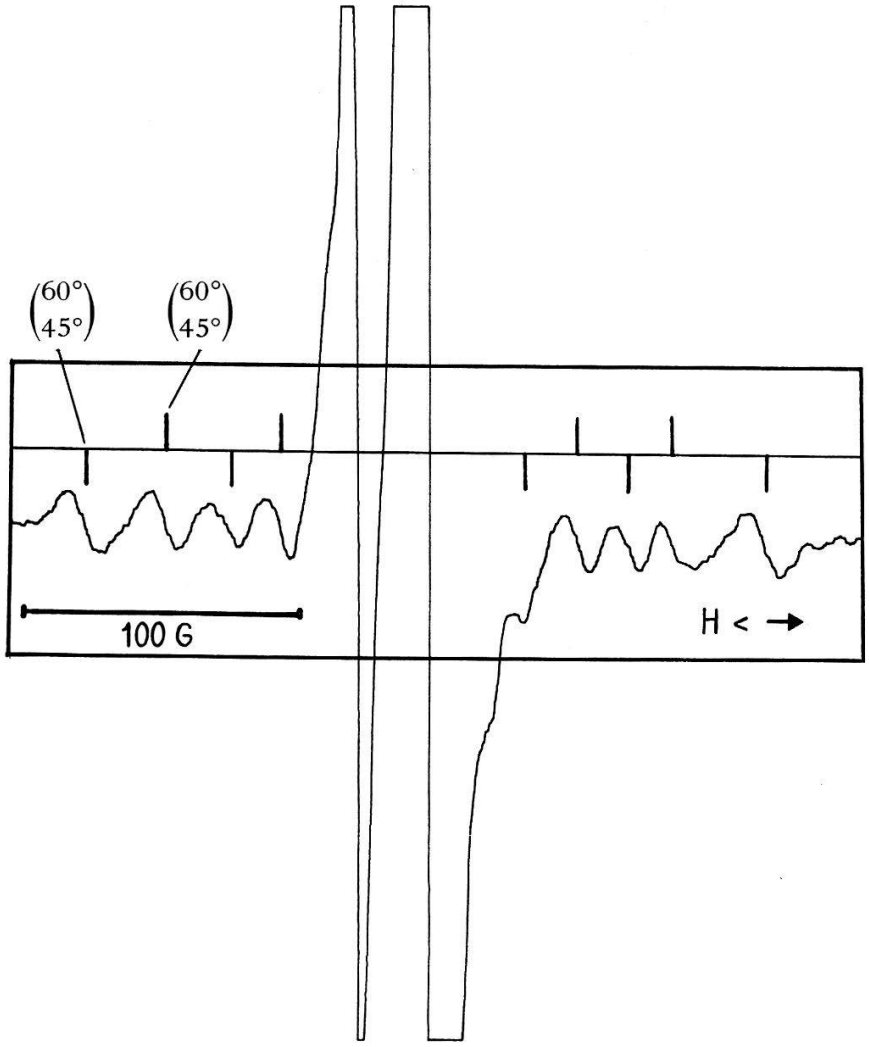

Figures 5a, b

Spectra of the ($Y^{16}O^{17}O$) centre in SrF_2. The strong lines are due to ($Y^{16}O_2$). The shfs interaction with the F^- nuclei is not resolved for any of the lines (due to a large $\vec{B}$ field modulation used). Fig. 5a: $\vec{B} \parallel [1, 1, 1]$. The two spectra of ($Y^{16}O^{17}O$) labelled $\vartheta = 35{,}3°$, $\varphi = 0°$ are centered on the low field line of ($Y^{16}O_2$) thus the corresponding $\vec{B}$ is parallel to the (x, z) plane of the (YO_2) centre. Fig. 5b: $\vec{B} \parallel [1, 1, 0]$. The two possible inequivalent locations of ^{17}O in the molecule involve two different spectra for $\vec{B}$ having the direction $\vartheta = 60°$, $\varphi = 45°$. Both they show only the ^{17}O sextett splitting.

The different models consistent with the spectra are depicted in Figures 6a, b, c. The first two represent essentially a molecule ion $(OF_2)^{3-}$ adjacent to a Y^{3+} ion and the third one is a $(YOF)^+$ structure. The ambiguities arise from the fact that yttrium has the same nuclear spin 1/2 as fluorine and that the two magnetic nuclei involved in the centre are not equivalent.

The centre is observed in crystals which have been slightly hydrolysed. When the oxygen concentration is enhanced by further hydrolysis this structure traps another oxygen ion and becomes the (YO_2) after X-raying of the crystal.

The actual symmetry of the centre is C_s. Thus the g tensor contains an asymmetric part (KNEUBÜHL [10]). But the differences between the measured components of $\boldsymbol{g}$ and the free electron g_e value are so small (see Table II) that this part

can be neglected. Thus the g matrix yields after diagonalization an orthorhombic tensor with respect to the principal axes (x, y, z) shown in Figure 9, which is to a very good approximation the actual one of the centre. Similar arguments apply to the hfs tensors.

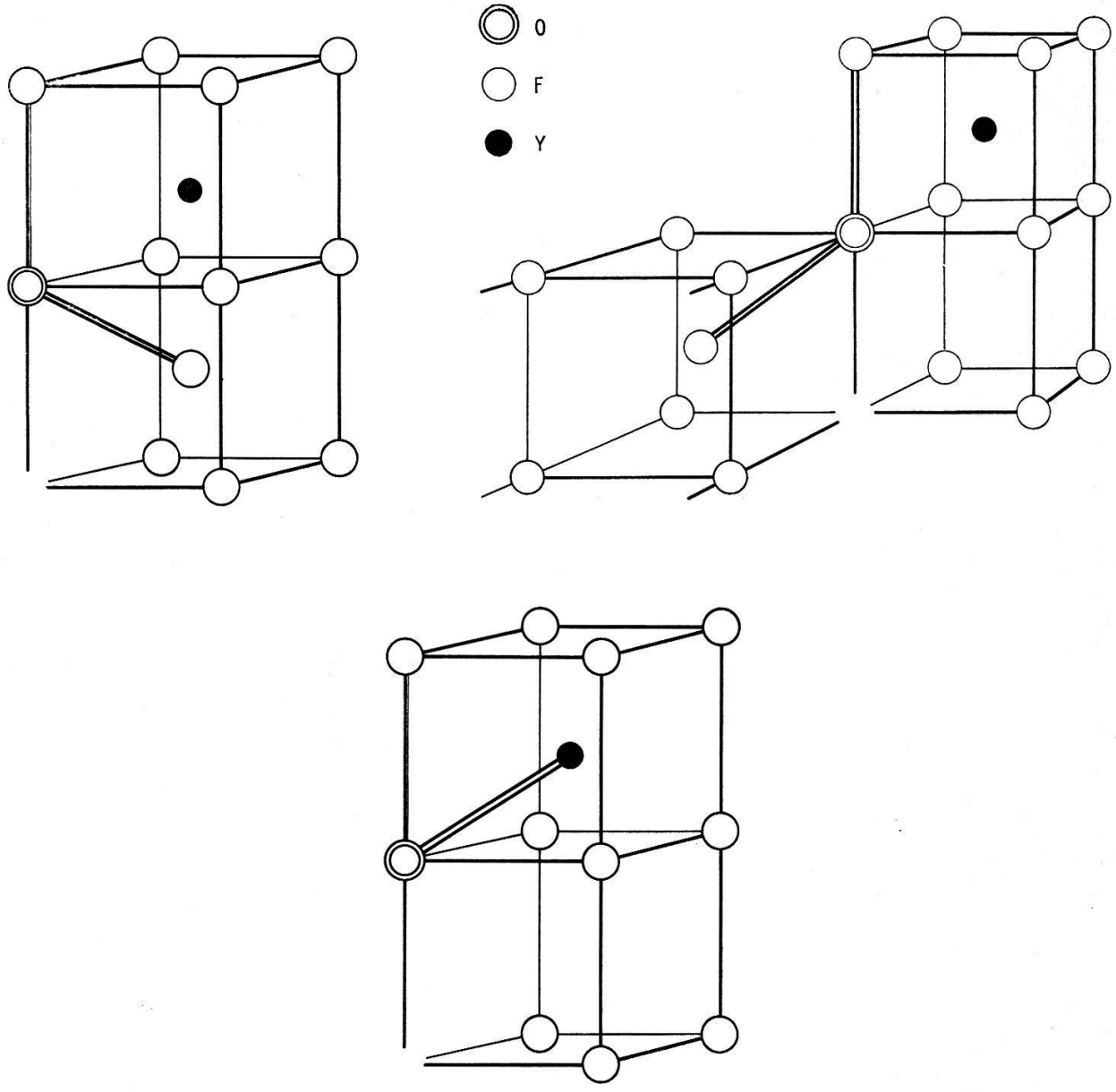

Figures 6a, b, c

Models of the centre having one oxygen ion implied.

Fig. 6a: The centre consists of a $(OF_2)^{3-}$ molecule ion. The interstitial F^- ion is in tetragonal location with respect to the yttrium ion. The centre together with the neighbouring yttrium ion and the vacancy involves one excedent positive charge unit ($1\ e^+$).

Fig. 6b: As 6a. The only difference consists in a different location of the interstitial F^- ion with respect to the foregoing model.

Fig. 6c: This model is a $(YOF)^{1+}$ structure. Thus the yttrium ion is implied in the centre. As in the foregoing cases the total resulting local charge is excedent positive ($1\ e^+$).

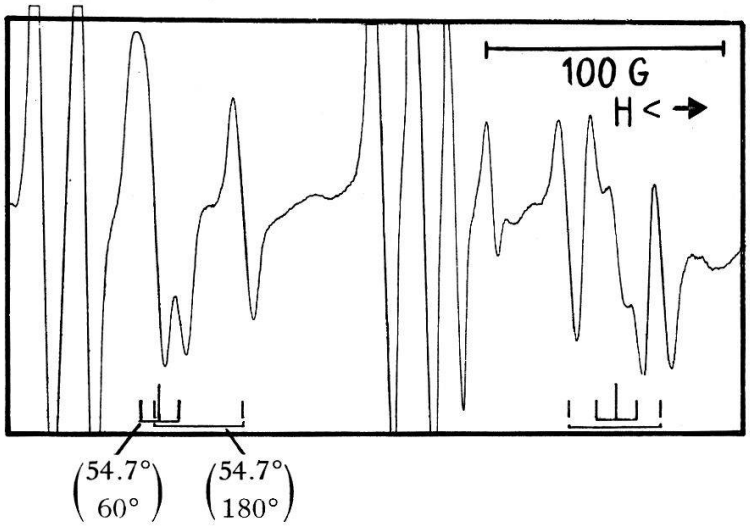

Figure 7

Spectrum of the centre having one oxygen ion implied. Host lattice: CaF_2, $T = 78\,°K$, $\vec{B} \parallel [0, 0, 1]$. The spectrum labelled $\vartheta = 54{,}7°$, $\varphi = 60°$ shows on the high field line the weak (and only for the given direction resolved) interaction with a supplementary nucleus of spin $^1/_2$. The lines not labelled arise from the V_K centre used to orient the crystal. The angles ϑ, φ, are defined in figure 9.

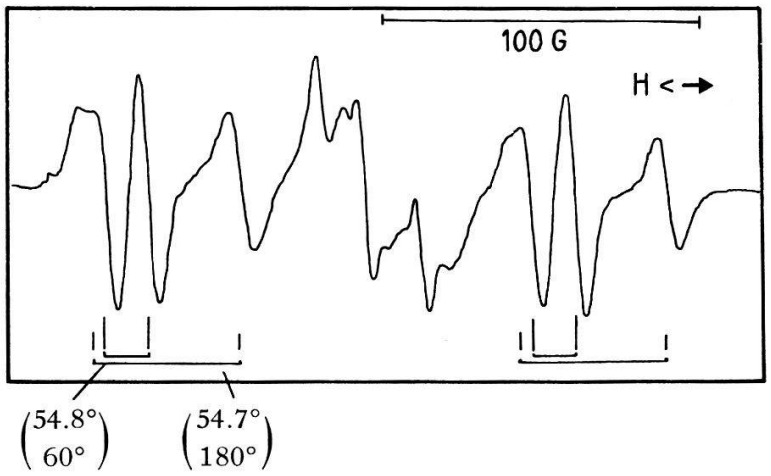

Fig. 8a: $\vec{B} \parallel [0, 0, 1]$. The spectrum labelled $\vartheta = 54{,}7°, \varphi = 180°$ corresponds to $\vec{B}$ being parallel to the principal axis of the tetragonal hfs whereas the other spectrum is due to $\vec{B}$ being perpendicular to this axis.

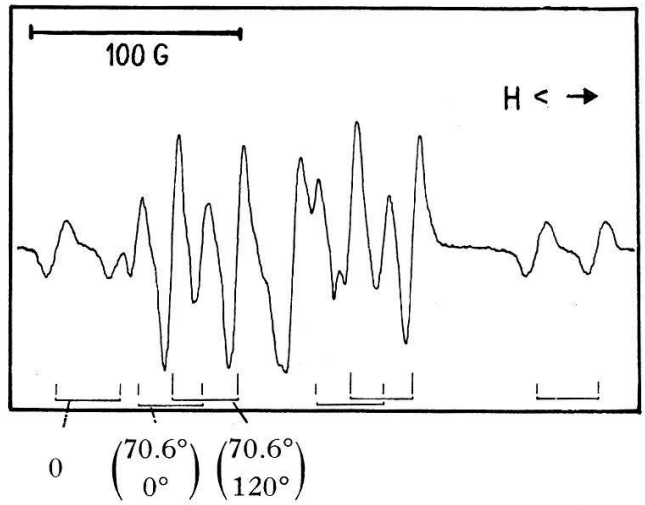

Fig. 8b: $\vec{B} \parallel [1, 1, 1]$. The two spectra labelled $\vartheta = 70{,}6°$, $\varphi = 0°$ respectively $\vartheta = 70{,}6°$, $\varphi = 120°$ do not coincide because their respective g value is different.

Figures 8a, b

Spectra of the centre having one oxygen ion implied. Host lattice: SrF_2, $T = 78\,°K$. See figure 9 for the definition of ϑ, φ.

The centre has 12 equivalent orientations in the host lattice which are all distinguishable by EPR. They are labeled by the corresponding directions of $\vec{B}$ with respect to *one* centre. Its reference coordinate system used is shown in Figure 9. The ***k*** axis points from the oxygen ion at [0, 0, 0] to the trigonally situated ion implied in the centre. The Figures 7 and 8a, b, c show the spectra corresponding to different special directions of $\vec{B}$.

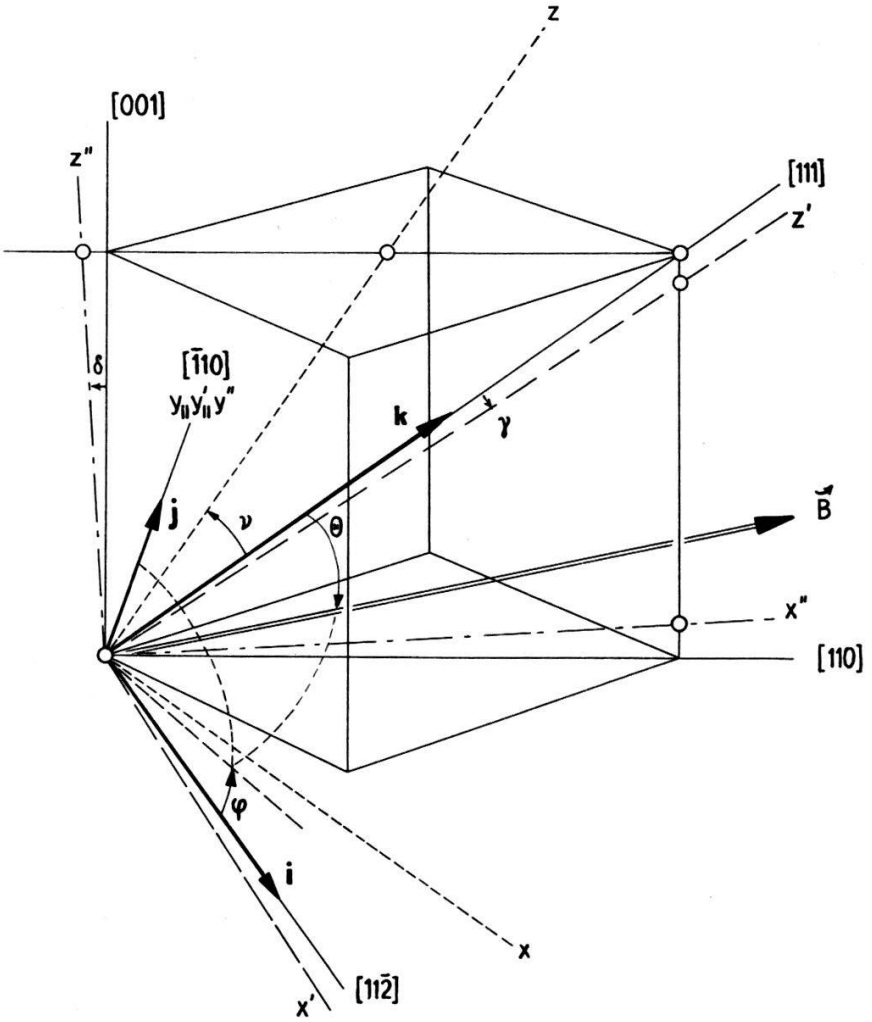

Figure 9

The principal axes of the different interactions of the centre having one oxygen ion implied are depicted as deduced from the EPR measurements. ***i***, ***j***, ***k*** are the reference axes of the centre, the oxygen ion being located at the origin. ϑ, φ describe the position of $\vec{B}$ with respect to those axes. x, y, z are the principal axes of **g**, x', y', z' are the ones of the trigonal hfs tensor (**A**) and x'', y'', z'' are the ones of the tetragonal hfs tensor (**B**).

Some preliminary ENDOR measurements on the centre in CaF_2 and in SrF_2 have been done to rule out a possible interstitial position of the oxygen ion. From the measurements the nuclear moment liable for the tetragonal hfs has been determined. It has been found to be the one of a fluoride ion. This result limits the possible simple models to the three given ones.

Quantitative Analysis of the EPR Spectra

The (YO_2) Molecule Ion

The Spin Hamiltonian

The following spin Hamiltonian was used to analyze the centres ($Y^{16}O_2$) and ($Y^{16}O^{17}O$)

$$\mathcal{H} = \mathcal{H}' + \mathcal{H}'' + \sum_{\mu} {}^{\mu}\mathcal{H}^F = \mathcal{H}_{\text{Zee}} + {}^{y}\mathcal{H} + {}^{1}\mathcal{H} + {}^{2}\mathcal{H} + \mathcal{H}'' + \sum_{\mu} {}^{\mu}\mathcal{H}^F . \qquad (1)$$

The terms are defined as follows. The nuclear Zeeman term is included in the hyperfine structure terms.

$$\mathcal{H}_{\text{Zee}} = \sum_{i=1}^{3} g_{ii}\, \beta\, B_i\, S_i \quad (S = 1/2) \text{ electronic Zeemannterm}$$

$${}^{y}\mathcal{H} = \sum_{i=1}^{3} {}^{y}A_{ii}\, S_i\, {}^{y}I_i - g_N^{y}\, \beta_N\, \vec{B} \cdot {}^{y}\vec{I} \quad ({}^{y}I = 1/2) \text{ yttrium hfs}$$

$${}^{1}\mathcal{H} = {}^{2}\mathcal{H} = \sum_{i=1}^{3} {}^{\alpha}A_{ii}\, S_i\, {}^{\alpha}I_i - g_N^F\, \beta_N\, \vec{B} \cdot {}^{\alpha}\vec{I} \qquad \alpha = 1, 2 \quad ({}^{\alpha}I = 1/2)$$

hfs due to the F^- nuclei 4, 5 (fig. 10)

$$\mathcal{H}'' = {}^{0}A_{\parallel}\, S_z'\, {}^{0}I_z' + {}^{0}A_{\perp}\, (S_x'\, {}^{0}I_x' + S_y'\, {}^{0}I_y') . \qquad {}^{17}\text{O hfs}$$

The above defined terms describe the resolved structures of the ordinary EPR spectra. The last term in (1) takes into account all the interactions seen only by ENDOR, to be discussed later.

The quadrupol term due to the ^{17}O nucleus has not been incorporated into $\mathcal{H}$ because its effect is negligible on the position of the allowed EPR lines. For the same reason the nuclear Zeeman term in $\mathcal{H}''$ has been omitted.

Determination of the Constants

The Hamiltonian $\mathcal{H}'$ which describes the spectra of the (YO_2) molecular centre is firstly considered. As justified by the EPR measurements it is assumed that all interactions can be referred to the same set of principal axes x, y, z (see Fig. 2). To obtain the eigenvalues of $\mathcal{H}'$ first order perturbation theory is applied by using the method given by BLEANEY [11] or CASTNER and KÄNZIG [3]. The experimental constants are listed in the Table I. By means of the ENDOR technique the determination of the yttrium and fluoride hfs constants (due to the nuclei labeled 4, 5 in Figure 10) have been completed. The resulting small tilt of the principal axes of the two fluorine hfs tensors is depicted in Figure 11.

The hfs tensor of ^{17}O has two of its principal axes tilted with respect to the ones of the interactions included in $\mathcal{H}'$. The resulting problem has been solved by transforming the whole Hamiltonian to the principal axes of the ^{17}O hfs tensor. The eigenvalues have then been computed by second order perturbation theory [11], assuming an isotropic g-factor and neglecting all nuclear Zeeman terms.

The experimental eigenvalues of the ^{17}O hfs tensor have been determined from the spectra with $\vec{B} \parallel [1, 0, 0]$, $\vec{B} \parallel [1, 1, 1]$ and $\vec{B} \parallel [1, 1, 0]$. To check the perturba-

Table I

Centre (YO_2)
Constants of the spin Hamiltonian of the interactions resolved in EPR
(hfs constants in Gauss)

Constants of $\mathcal{H}$ (formula 1)	Host lattice CaF_2	SrF_2	Nucleus (figure 10)
g_x	2,0037 ± 0,0008	2,0033 ± 0,0008	
g_y	2,0264 ± 0,0008	2,0287 ± 0,0008	
g_z	2,0118 ± 0,001	2,0084 ± 0,001	
$\lvert {}^1A_x\rvert = \lvert {}^2A_x\rvert$	18,67 ± 0,05[a])	9 ± 1,5	
$\lvert {}^1A_y\rvert = \lvert {}^2A_y\rvert$	5,20 ± 0,03[a])	$\leqslant 2$	F^-
$\lvert {}^1A_z\rvert = \lvert {}^2A_z\rvert$	4,95 ± 0,03[a])	$\leqslant 2$	(numbers 4, 5)
β	4,5 ± 1,5°		
$\lvert {}^yA_x\rvert$	4,11 ± 0,04[a])	4,04 ± 0,08[a])	
$\lvert {}^yA_y\rvert$	3,96 ± 0,04[a])	3,80 ± 0,08[a])	Y
$\lvert {}^yA_z\rvert$	4,27 ± 0,04[a])	4,19 ± 0,08[a])	(number 1)
$\lvert {}^0A_{\eta_3}\rvert = \lvert {}^0A_{\parallel}\rvert$	72,7 ± 1,1	71,9 ± 1,1	
$\lvert {}^0A_{\eta_2}\rvert = \lvert {}^0A_{\perp}\rvert$	6 ± 2,5	5 ± 2,5	^{17}O
$\lvert {}^0A_{\eta_1}\rvert = \lvert {}^0A_{\perp}\rvert$	6 ± 2,5	5 ± 2,5	(numbers 2, 3)
δ_0	10 ± 1,5°	10,5 ± 1,5°	

[a]) Values obtained from ENDOR measurements.

tion calculation we diagonalized the Hamiltonian $\mathcal{H}' + \mathcal{H}''$ for different directions of $\vec{B}$ on a computer by inserting the experimental constants. The results agree with the ones of the perturbation calculation within the errors of measurements.

The constants of $\mathcal{H}''$ are given in Table I too.

Electronic Structure

Inspection of the Table I shows that the magnitude of the hfs of ^{17}O and Y do not depend upon the spacing, a_0, of the lattice, indicating the strongly molecular character of the centre. On the other hand the hfs of the two fluorine ions (4 and 5 in Figure 10) shows a strong dependence on a_0 indicating them being lattice ions. The entity of the molecule is thus formed by the complex (YO_2).

However, it cannot be excluded that the cation located on the other side of the O_2^{3-} molecule ion (number 18 in Figure 10) is also contained in the molecular complex which is described in this case by $(CaYO_2)^{2+}$ respectively $(SrYO_2)^{2+}$. A reliable quantitative answer would possibly be obtained from the measurements of the hfs splitting of the isotope ^{43}Ca or ^{87}Sr in the spectrum of the centre (which has not yet been done). A preliminary rough indication is obtained by summing up the probability of presence of the magnetic electron on the ions forming the (YO_2) group. The calculated figure is 1.2. The probability of presence of the magnetic electron on the cation 18 is thus probably small. Taking further into account the small variation of the EPR parameters of the centre as a function of the host crystal we consider tentatively the cation 18 as belonging to the lattice.

The angle δ_0 giving the tilt of the p function of the oxygen ions with respect to the x axis of the centre is remarkably small. Thus the structure of the (YO_2) centre is

nearer the form ($Y^{3+} - O_2^{3-}$) than the shape (O–Y–O). The (YO_2) is somewhat related to a V_F centre strongly associated with an yttrium ion. The host lattice acts mainly on the excited states of the molecule through the crystal field, producing the observed lattice spacing dependence of the magnitude of g and of the energy of the optical transitions.

A semiquantitative description of the (YO_2) ground state will now be given by using the superficial similarity between the (YO_2) and a V_F centre. The unperturbed O_2^{3-} has the same number of electrons as the F_2^- V_k centre (KÄNZIG et al. [3]), and its electronic levels correspond to those of the F_2^- with perhaps different order of some of them. Within the frame of the LCAO approximation the orbitals are constructed from the 1 s, 2 s, 2 p functions of the two ions involved.

The low symmetry crystals field reduces the D_∞ symmetry of the free O_2^{3-} to C_{2V} thus permitting some mixing of part of the $|p\,\pi\rangle$ functions into the $|p\,\sigma\rangle$ orbitals. The state of the magnetic electron is described by

$$|M\rangle \propto (\alpha\,|p\,\sigma\rangle + \beta\,|p\,\pi\rangle + \gamma\,|s\rangle\,. \tag{3}$$

It transforms as B_1 of C_{2V}. The greek letters are mixing coefficients and the different parts are the following ones (neglecting overlap):

$$\begin{aligned} |p\,\sigma\rangle &= \frac{1}{\sqrt{2}}\,(|x,2\rangle + |x,3\rangle)\,,\\ |p\,\pi\rangle &= \frac{1}{\sqrt{2}}\,(-|z,2\rangle + |z,3\rangle)\,,\\ |s\rangle &= \frac{1}{\sqrt{2}}\,(|s,2\rangle - |s,3\rangle)\,. \end{aligned} \tag{4}$$

The numbers in the kets refer to the number of the ions as given in Figure 10 and x means a p_x function etc. The coordinate axes are defined in Figure 2.

This ground state is not complete. As has been discussed before, the yttrium ion is also part of the centre. Consequently one has to consider some admixture of an yttrium wave function which must have the same symmetry B_1 as $|M\rangle$. The only allowed functions are $n\,p_x$ and linear combinations of $n\,d$ or $n\,f$ orbitals – but no s function. Thus this approach cannot explain the observation of an yttrium hf interaction which is almost isotropic. Obviously a one-determinantal description of the ground state is inadequate and one has to take into account configuration interaction (see eg. HEINE [12]).

On the other hand the state of the magnetic electron (3) permits to calculate the ^{17}O hfs interaction as the contribution of the yttrium wave function is small.

One obtains after transformation of $\mathcal{H}''$ to its principal axes η_1, η_2, η_3 (all overlaps neglected)

$$^0A_\parallel = A_s + 2\,A_p \quad \Big| \quad A_s = g_N\,\beta_N\,\gamma^2\,\frac{4\pi}{3}\,|\psi_s(0)|^2 \tag{5}$$

$$^0A_\perp = A_s - A_p \quad \Big| \quad A_p = g_N\,\beta_N\,(\alpha\cos\delta_0 + \beta\sin\delta_0)^2\,\frac{1}{5}\left\langle\frac{1}{r^3}\right\rangle_{2p}\,. \tag{6}$$

This approach leads to the following relation for the tilt angle: $\mathrm{tg}\,\delta_0 = \beta/\alpha$. Inserting the experimental values one obtains $\beta/\alpha = 0.176$. With the aid of this value and

$\langle 1/r^3 \rangle_{2p} = 3.36 \times 10^{25}$ cm^{-3} for 2 p oxygen functions of the restricted HF type (13), the coefficient α^2 was calculated from (6). The value thus obtained is $\alpha^2 = 0.86$.

The probability to find the electron on the yttrium ion can roughly be estimated by comparing the yttrium hfs splitting of the centre to the isotropic part of the hfs splitting of Y^{2+} in $SrCl_2$ (obtained from our measurements) if it is assumed that a 4 d orbital gives the main contribution to the yttrium part of the ground state of (YO_2). Thus in the simple model given one supposes the core polarization mechanism being alike for the Y^{2+} state of the yttrium ion either being included in the centre or incorporated substitutionally into the matrix $SrCl_2$. The probability turns out to be 0.14.

The sum of the square of the coefficients of (3) together with the probability estimated for yttrium gives a value of about 1.2.

Quantitative Analysis of the Centre Involving One Oxygen Ion

Hamiltonian and Quantitative Analysis of the Spectra

The ansatz of the spin Hamiltonian is

$$\mathcal{H} = \mathcal{H}_{\text{Zee}} + \mathcal{H}_{\text{trig}} + \mathcal{H}_{\text{tetr}} . \tag{7}$$

The different contribution are defined by

$$\mathcal{H}_{\text{Zee}} = \sum_i g_{ii} B_i S_i \quad (S = 1/2) \text{ electronic Zeemann term}$$

$$\mathcal{H}_{\text{trig}} = \sum_i A_{ii} S_i' I_i' - g_N^{\text{trig}} \beta_N \vec{B} \cdot \vec{I} \quad (I = 1/2) \text{ trigonal hfs}$$

$$\mathcal{H}_{\text{tetr}} = \sum_i B_{ii} S_i'' J_i'' - g_N^{\text{tetr}} \beta_N \vec{B} \cdot \vec{J} \quad (J = 1/2) \text{ tetragonal hfs} .$$

The principal axes of the three tensors **g**, **A**, **B** do not coincide. For convenient diagonalization of the Hamiltonian, it has been transformed to the axes x, y, z of Figure 9. Then the solutions have been found by second order perturbation theory and also by computer diagonalization of the matrix. In the Figure 9 are depicted the principal axes of the tensors **g**, **A**, **B** and in Table II are listed their eigenvalues and the angles defined in Figure 9.

The axes of **A** are defined by (x', y', z') and the ones of **B** by (x'', y'', z''). It is most remarkable to notice how much the hyperfine structures **A** and **B** vary with the lattice dimensions. This is to be contrasted to the constant hfs of the ^{17}O isotope and of the Y^{3+} ion in the (YO_2) structure. The centre considered here is a much less rigid structure, and it is much more alike an oxygen ion O^- subjugated to a crystal field of low symmetry and being in pronounced hfs interaction with two neighbours. The probability of presence in the 2 p state of each of the neighbours is 2.1% for the one in tetragonal direction and 19% for the trigonally located one, if both are fluoride ions and if the same sign of all the components of each of the hfs tensors are assumed. If, instead, the nucleus in trigonal position is an yttrium ion a probability of presence of about 200% is calculated when the electron is supposed to be located in a 4 d orbital. The $\langle 1/r^3 \rangle_{4d} = 9.25 \times 10^{25}$ cm^{-3} used to estimate the given figure was obtained from a theoretical calculation and is rather an overestimation (BARNES et al. [14]). About the

same amount is found, when the electron is located in a 4 p orbital. This value seems so high, that it is rather improbable to have an yttrium ion in trigonal location (Fig. 6c).

Table II

Centre involving one oxygen ion.
Constants of the spin Hamiltonian of the centre obtained from the EPR results
(hfs constants in Gauss)

Constants of $\mathcal{H}$ (formula 7)	Host lattice CaF_2	SrF_2	Nucleus
g_x	2,0244 ± 0,002	2,0239 ± 0,002	
g_y	2,0233 ± 0,0015	2,0180 ± 0,002	
g_z	2,0028 ± 0,0015	2,0027 ± 0,0015	
$\sphericalangle (z, \boldsymbol{k}) = \nu$	11,5 ± 2,5°	20,5 ± 2,5°	
$\lvert A_x \rvert$	56 ± 2	41,5 ± 1,5	
$\lvert A_y \rvert$	53,5 ± 2	37,5 ± 1,5	F or Y
$\lvert A_z \rvert$	308,6 ± 0,8	228,3 ± 0,8	
$\sphericalangle (z', \boldsymbol{k}) = \gamma$	2,5 ± 1°	0 ± 1°	
$\lvert B_x \rvert$	9 ± 2	11 ± 1,5	
$\lvert B_y \rvert$	8 ± 2	13,9 ± 1,5	F
$\lvert B_z \rvert$	37,2 ± 0,8	50,1 ± 0,8	
$\sphericalangle (z'', C_4) = \delta$	2 ± 1,2°	2,7 ± 1,2°	

Endor Investigation of the Superhyperfine Structure (shfs) of the Centre ($Y^{16}O_2$)

Symmetry considerations

In the Figure 10 the centre is depicted as being placed in a fragment of a perfect crystal lattice. The overall point symmetry group of this complex is C_{2V} with respect to x, y, z. The classification according to symmetry of the nuclei yields the sets having

Table III

Some of the sets of nuclei obtained by applying the transformations of the group C_{2V} to the centre (YO_2) and its surroundings (see Figure 10)

Lable	Nuclei	Coordinates of the nuclei with respect to x, y, z of Figure 10	Type of set (table IV)
1	Y	$(0, 0, \sqrt{2}/4\, a)$	m_0
2, 3	O	$(\pm\, a/4, 0, 0)$	m_{xz}
4, 5	F	$(\pm\, 3\, a/4, 0, 0)$	m_{xz}
6	F	$(\pm\, 5\, a/4, 0, 0)$	m_{xz}
8	F	$(\pm\, a/4, \pm\, \sqrt{2}\, a/4, +\sqrt{2}\, a/4)$	m
10	F	$(\pm\, a/4, \pm\, \sqrt{2}\, a/4, -\sqrt{2}\, a/4)$	m
9	F	$(\pm\, a/4, \pm\, \sqrt{2}\, a/2, 0)$	m
14	F	$(\pm\, 3\, a/4, \pm\, \sqrt{2}\, a/2, 0)$	m
13	F	$(\pm\, 3\, a/4, \pm\, \sqrt{2}\, a/4, +\sqrt{2}\, a/4)$	m
15	F	$(\pm\, 3\, a/4, \pm\, \sqrt{2}\, a/4, -\sqrt{2}\, a/4)$	m

the same eigenvalues of their shfs tensors. The nuclei belonging to one given set are labeled by the same number in the figure and in Table III some of the sets are listed.

Due to the given symmetry all the sets are further classified into the four types given in Table IV (HERZBERG [15], KNEUBÜHL [10]). The essential point is that to each of the types corresponds a different structure of the shfs matrix with respect to the symmetry axes.

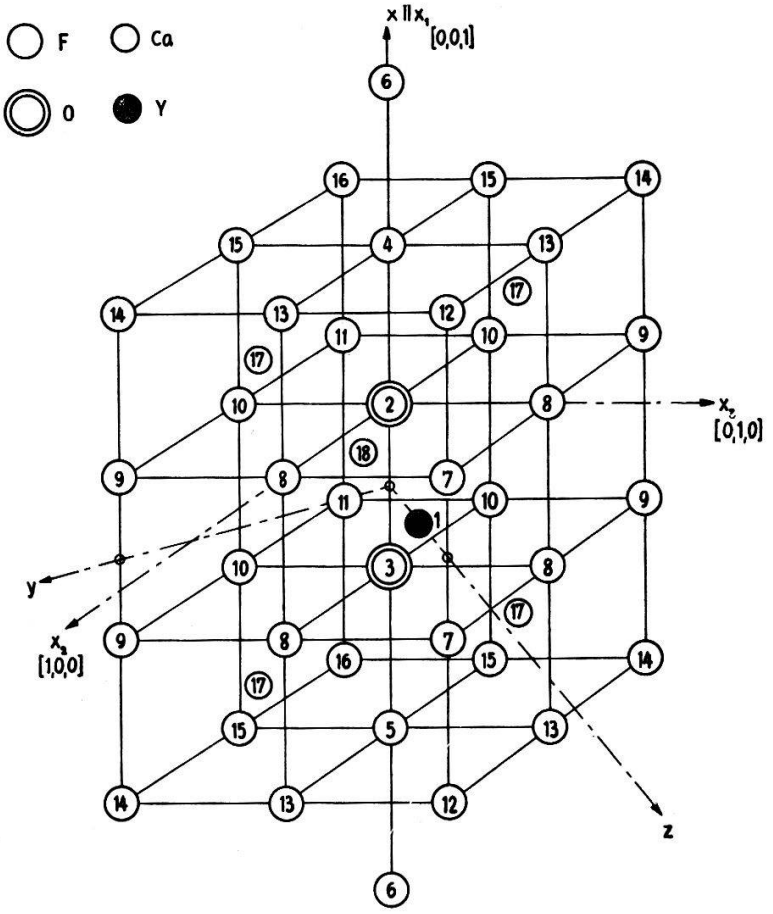

Figure 10

Fragment of an ideal CaF_2 crystal having a (YO_2) centre incorporated. Nuclei which transform one into the other under the group C_{2V} are labelled the same label (except the centre and the nuclei 4, 5).

The symmetry of the given model has been deduced from the EPR spectra. The whole of the ENDOR spectra confirmed it to be C_{2V} (the only exception – observed in the spectra of the nuclei 4, 5 – is due to magnetic exchange effects as will be shown below).

The given results do not allow to exclude the possibility of defects (missing fluoride ions, substitutional oxygen ions) located in the next nearest neighbourhood or in some distance of the centre. To solve this problem one would have to evaluate the change of the shfs tensor of each of the different nuclei forming a given set when this set is destroyed by introducing a defect. The necessary detailed investigation has not been

done. Defects in direct neighbourhood of the centre can on the other hand be excluded from the EPR measurements.

The structure of the matrix of each of the observed shfs interactions is obtained from the spectra (thus the symmetry classification of Table IV furnishes valuable help in the identification of the underlying sets of nuclei). However, it can only be determined within some sign ambiguities of the nondiagonal matrix elements from the experiments as is easily shown by elementary symmetry arguments. Thus for a given nucleus belonging to a set of the type m_{xz}, m_{yz} or m the eigenvectors of the shfs tensor are not uniquely determined. The eigenvalues with their relative signs, however, are obtained unambiguously. This result together with their special position implies for the nuclei 8, 10 that one is not able to point out from the spectra which one of the shfs tensor components is directed to the centre.

Table IV

Type	Number of nuclei forming the set	Number of components of the shfs tensor	Coordinates of the nuclei (in figure 10)
m_0	1	3	$(0, 0, z)$
m_{xz}	2	4	$(\pm x, 0, z)$
m_{yz}	2	4	$(0, \pm y, z)$
m	4	5	$(\pm x, \pm y, z)$

It has been pointed out (eg. by KNEUBÜHL [10]) that the shfs tensors are asymmetric if the local point symmetry group at the sites of the underlying nuclei is sufficiently low. But actually the asymmetry can be neglected in any of the cases considered as the orbital moment of the centre is almost quenched and as the shfs interactions involved are small.

Qualitative Discussion of the ENDOR Spectra

The sets 8 and 10 (Figure 10) are inequivalent due to the fact that (x, y) is not a mirror plane of the centre. Part of the angular plot of their ENDOR spectra is given in Figure 12a. A priori it is not possible to correlate the two spectra to their respective set as both spectra are always observed together. Detailed ab initio claculations would in principle give a solution of this problem, but as the actual geometry of the neighbourhood of the centre is not known none have been performed. The same problems arise also for the sets 13 and 15. Due to strong overlap of the lines their spectra have only partly been identified.

The ENDOR lines of the sets 12 and 16 are hidden in the centre part of the spectra. Nevertheless it can be shown that their shfs constants are smaller than the ones of the set 14, whose angular plot of the spectrum is given in Figure 12b together with the one of the set 9. Probably the cations 17 being polarized by the centre produce an amplified shfs interaction at the nuclei 14.

Spin Hamiltonian

For quantitative analysis of the spectra the spin Hamiltonian of the formula (1) is used

$$\mathcal{H} = \mathcal{H}' + \sum_{\mu} {}^{\mu}\mathcal{H}^{F}\,(S, {}^{\mu}I) \tag{1}$$

with

$${}^{\mu}\mathcal{H} = \sum_{i} ({}^{\mu}A_{ii}\, S_i\, {}^{\mu}I_i - g_N^{\mu}\, \beta_N\, \vec{B} \cdot {}^{\mu}\vec{I}) \tag{9}$$

μ sums over all nuclei showing resolved shfs interaction except the nuclei 4, 5. The index i enumerates the principal axes of each tensor ${}^{\mu}\mathbf{A}$. The approximation of independent nuclear spins is valid for all the ${}^{\mu}\mathcal{H}$. Thus the eigenvalues are obtained by individual diagonalization of each of them. The solution is given by (${}^{\mu}\mathbf{A}$ is orthorhombic, $\mathbf{g}$ is supposed to be isotropic)

$$\begin{aligned} {}^{\mu}\varepsilon(M_s, m_{\mu}) = m_{\mu} \{&(M_s\, {}^{\mu}A_{11} - g_N^{\mu}\, \beta_N\, B)^2\, n_1^2 + (M_s\, {}^{\mu}A_{22} - g_s^{\mu}\, \beta_N\, B)^2\, n_2^2 \\ &+ (M_s^{\mu}\, A_{33} - g_N^{\mu}\, \beta_N B)^2\, n_3^2\}^{1/2} \end{aligned} \tag{10}$$

n_1, n_2, n_3 are the cosines of the angles of $\vec{B}$ with respect to the principal axes of ${}^{\mu}\mathbf{A}$.

The total energy is given by

$$E = \varepsilon_{\mathrm{Zee}}(M_s) + \sum_{\mu} {}^{\mu}\varepsilon(M_s, m_{\mu})\ . \tag{11}$$

From this formula the ENDOR and EPR transitions are obtained by introducing the well-known selection rules. It is important to notice that ${}^{\mu}\mathcal{E}$ of (10) and E of (11) depend on the relative signs of the components of ${}^{\mu}\mathbf{A}$. The formula (10) has been obtained by the use of a modification of the method given by BLEANEY [11] or CASTNER and KÄNZIG [3].

Quantitative Analysis of the ENDOR Spectra

The constants of some of the identified spectra have been evaluated by fitting the formula 11 to their angular plot. The parameters thus obtained are listed in Table V.

In the Figure 11 the hfs tensor axes of the isotope ^{17}O and the shfs ones of the neighbouring fluoride ions located on the x axis are depicted. Furthermore the s and p functions contributing to the LCAO molecular orbital of the magnetic electron are shown. Remark that the tilt angle between the axis of the p functions and the x axis diminishes when the series of nuclei 2, 4, 6 is considered in this order. The $p\,\pi$ part of the orbital is 'damped out'. However, it cannot be concluded that the $p\,\pi$ part of overlap is solely responsible for the bending of the wave function. There might also be a contribution due to the shifted position of the different ions involved.

The shfs tensor axes of the sets 8 and 10 are not uniquely labeled. The following rather qualitative arguments will show that probably the component A_2 of their shfs tensor is pointing to the centre (A_2 and A_3 are in competition). CLOGSTON et al. [16] and SHULMAN and SUGANO [17] (and others who have treated appropriate cases)

who have investigated the systems ZnF_2: M_n^{2+} respectively $KNiF_3$ by EPR and NMR have calculated the different contributions to the shfs tensor of the F^- ligands in those cases. The contributions consist of a transferred part one due to overlap between the central ion and the ligands considered and a part corresponding to the classical dipol-dipol interaction.

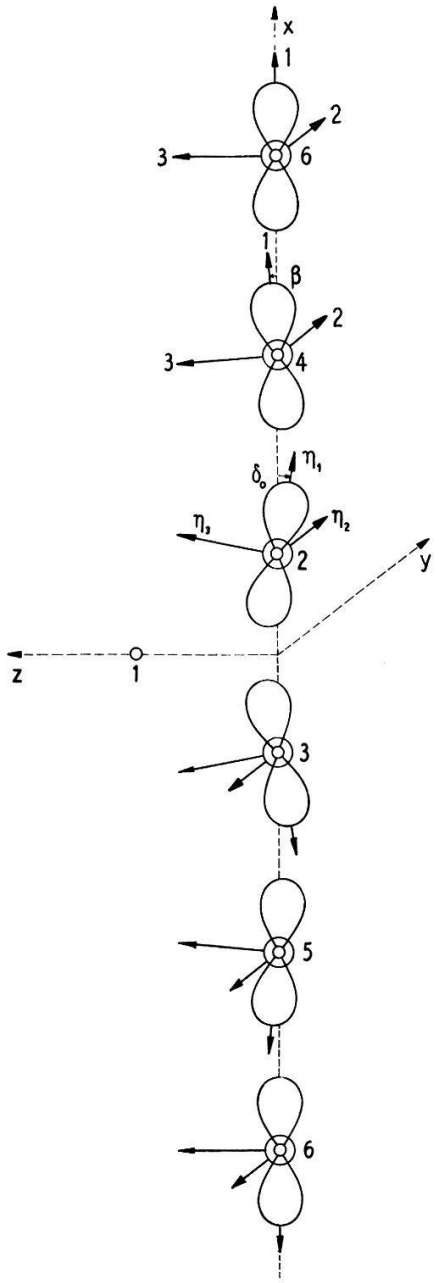

Figure 11

The figure shows the principal axes of the ^{17}O hfs interaction and of the shfs interactions of the centre (YO_2) with different F^- nuclei located on the x axis. The atomic s, p orbitals shown contribute to the ground state of the magnetic electron.

This model is applied to the present case by using rough approximations. The shfs tensors (given in Table V) are decomposed into a contact term and an axially symmetric p part both due to transferred shfs and further an axially symmetric dipol-dipol contribution having its symmetry axis pointing along the eigenvector labeled by A_1. This decomposition yields for both sets that A_2 is pointing to the centre.

MIEHER et al. [18] in their paper on the ENDOR of the H-centre determined the signs of the isotropic part of the different shfs tensors from the dipol-dipol interaction with the centre. Application of this argument to the sets analyzed at present yields the signs given in Table V for the sites 8, 9 and 10. The shfs tensor components of the set 14 could not be determined with sufficient precision to get useful information about the dipol-dipol coupling.

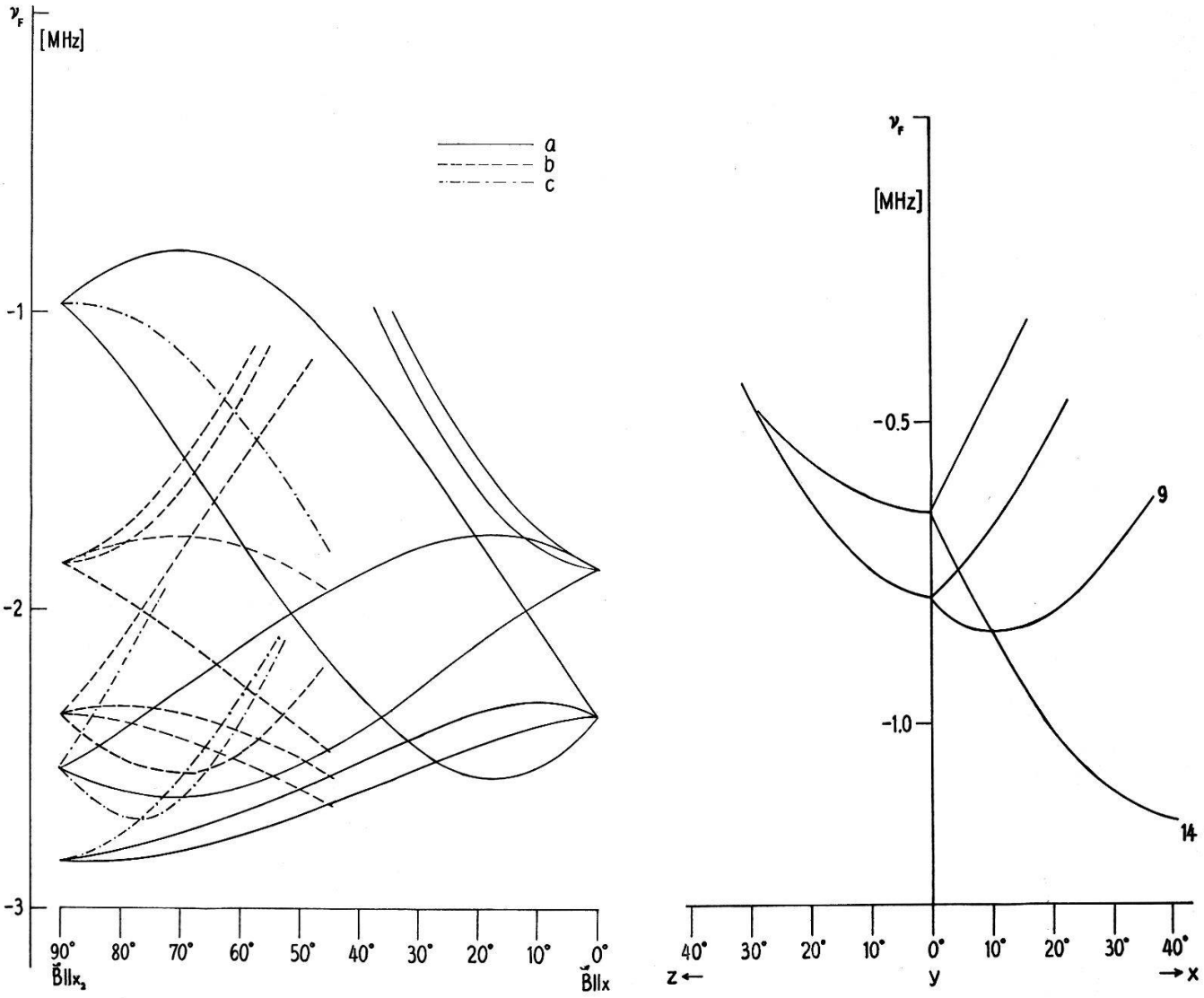

Figures 12a, b

Angular plots of some of the experimental ENDOR spectra of the (YO_2) centre in CaF_2. Only the lines with $^{\mu}\nu < \nu_F$ are considered. Experimental points every 2.5° (not shown).

Fig. 12a: $\vec{B} \parallel (1,0,0)$. The spectrum arises from the nuclei 8, 10. The ordinary spectrum is labelled *a*. Due to strong overlap of the EPR lines, part of the angular plot of the spectrum with $\vec{B} \parallel (y, z)$ is observed simultaneously (labelled *b*). When $\vec{B}$ is approaching x_2 or x_3 the spectrum with $\vec{B}$ approaching x is also observed (labelled *c*) due to overlap of the lines.

Fig. 12b: The spectrum is due to the nuclei 9, 14. $\vec{B} \parallel (x, y)$ and $\vec{B} \parallel (y, z)$.

Table V

Principal values and directions of the shfs tensors measured by ENDOR

Nuclei	Principal values of the shfs tensors (in MHz)[a]			Angles of the principal axes with respect to x, y, z[a]			Isotropic part of
(Figure 10)	A_1	A_2	A_3	φ	ϑ	ψ	the shfs tensors A_s
1	$\pm 11{,}521 \pm 0{,}01$	$\pm 11{,}112 \pm 0{,}01$	$\pm 11{,}956 \pm 0{,}01$	$0 \pm 1°$	$0 \pm 1°$	$0 \pm 1°$	$(\pm)$ 11,532
4, 5	$\pm 52{,}32 \pm 0{,}12$	$\pm 14{,}57 \pm 0{,}08$	$\pm 13{,}88 \pm 0{,}08$	$90°$	$\pm 4{,}5 \pm 1{,}5°$	$-90°$	$(\pm)$ 29,23
6	$\pm 1{,}23 \pm 0{,}01$	$\pm 0{,}09 \pm 0{,}01$	$\pm 0{,}09 \pm 0{,}03$	$0 \pm 2°$	$0 \pm 1°$	$0 \pm 2°$	$(\pm)$ 0,35
8, 10[a]	$-5{,}068 \pm 0{,}035$	$-1{,}632 \pm 0{,}035$	$-5{,}737 \pm 0{,}035$	$-16{,}1 \pm 1{,}5°$	$+45{,}1 \pm 1{,}5°$	$-7{,}9 \pm 1{,}5°$	$(-)$ 4,146
	$-3{,}557 \pm 0{,}035$	$+0{,}719 \pm 0{,}035$	$-5{,}600 \pm 0{,}035$	$-29{,}8 \pm 1{,}5°$	$+54{,}8 \pm 1{,}5°$	$+22{,}8 \pm 1{,}5°$	$(-)$ 2,813
9	$-0{,}46 \pm 0{,}15$	$+1{,}629 \pm 0{,}01$	$-1{,}045 \pm 0{,}02$	$\pm 10{,}5 \pm 3°$	$0 \pm 2°$	$0 \pm 2°$	$(+)$ $0{,}041 \pm 0{,}06$
14	$\pm 0{,}05 \pm 0{,}15$	$\pm 2{,}308 \pm 0{,}02$	$\pm 0{,}24 \pm 0{,}25$	$\pm 40 \pm 3{,}5°$	$0 \pm 3°$	$0 \pm 2°$	$(\pm)$ 0,678

[a]) The correlation between the old and the new axes is given by $x \rightarrow A_1$, $y \rightarrow A_2$, $z \rightarrow A_3$ the new axes being designed by their corresponding shfs tensor component.

[a]) Goldstone's convention is used with respect to the axes x, y, z of the centre.

[a]) The three other tripletts of signs of the Eulerian angles are obtained from the given ones by applying the transformations of C_{2V} to them. Under the assumption that A_2 is pointing towards the centre the given sign of the Eulerian angles corresponds to the nuclei specified by ($x > 0$, $y > 0$, $z > 0$) or ($x < 0$, $y < 0$, $z < 0$).

Quantitative Analysis of the Indirect Nuclear Magnetic Coupling Between the Nuclei 4 and 5

The ENDOR lines due to the nuclei 4 and 5 in the spectra taken with $\vec{B} \parallel y$ and $\vec{B} \parallel z$ show a doublett-splitting (Fig. 13) which is not explained by the actual symmetry of the complex. The following analysis taking advantage of the ideas of RAMSAY and PURCELL [19] will show that magnetic exchange effects are at the origin of this splitting.

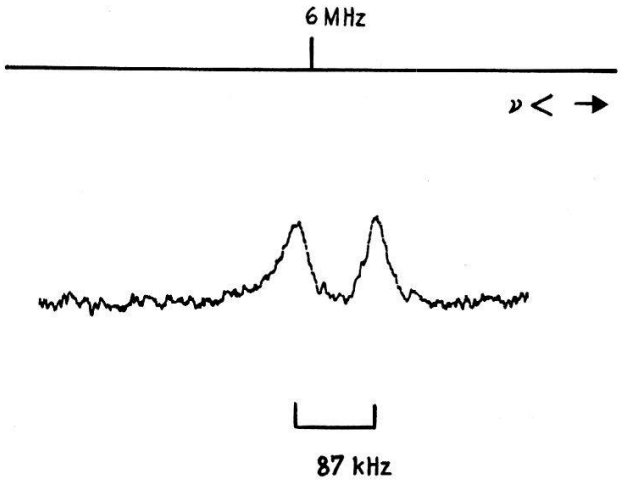

Figure 13

One of the ENDOR lines (determined by $^{\mu}\nu < \nu_F$) of the shfs interaction with the equivalent F^- nuclei 4, 5 (Figure 10) is shown, $\vec{B} \parallel y$. The doublett splitting (87 kH_2) arises from the indirect coupling between the two nuclear magnetic moments. $\nu_F = 13.317$ MHz.

Due to the shfs interaction each of the two nuclear moments splits the Zeeman levels of the magnetic electron of the centre. At the same time it modifies the corresponding electronic wave functions. The other nucleus interacts with the perturbed electronic states. The interaction is analyzed by the sub Hamiltonian $\overline{\mathcal{H}} = {}^1\mathcal{H} + {}^2\mathcal{H}$, taken from equation (1). $\overline{\mathcal{H}}$ is first diagonalized in the electron spin functions giving an operator $\overline{\overline{\mathcal{H}}}$ respectively $\overline{\overline{h}}$ acting only on the nuclear spin states.

$$\overline{\overline{\mathcal{H}}} = \langle M_s | {}^1\mathcal{H} | M_s \rangle + \left\{ - \frac{\langle M_s | {}^1\mathcal{H} | M'_s \rangle}{E_{M'_s} - E_{M_s}} \langle M'_s | + \langle M_s | \right\} \times {}^2\mathcal{H} \left\{ | M_s \rangle - | M'_s \rangle \frac{\langle M'_s | {}^1\mathcal{H} | M_s \rangle}{E_{M'_s} - E_{M_s}} \right\}$$

$$M_s, M'_s = \pm 1/2 \qquad E_{M_s} = g_e \beta B M_s \qquad E_{M'_s} - E_{M_s} = \Delta E = h \nu_M$$

only the following expressions are kept

$$\overline{\overline{\mathcal{H}}} \simeq \overline{\overline{h}} = \langle M_s | {}^1\mathcal{H} + {}^2\mathcal{H} | M_s \rangle - \frac{\langle M_s | {}^1\mathcal{H} | M'_s \rangle \langle M'_s | {}^2\mathcal{H} | M_s \rangle + c\,c}{\Delta E} \tag{12}$$

$\overline{\overline{h}} = \overline{\overline{h}}({}^1I, {}^2I)$. Its eigenvalues are calculated by using the method given by MCCONNELL et al. [20]. It is assumed that the shfs tensor of both nuclei is axially symmetric with the x axis (Fig. 10) being the symmetry axis.

For $\vec{B}$ lying in the (y, z) plane the calculated frequencies are[1])

$$\nu'_{\pm} = \left| + \frac{1}{2} A_{\perp} - \nu_F \pm \frac{1}{8\nu_M} ({}^1A_{\parallel}^2 + {}^1A_{\perp}^2) \right|$$

$$\nu''_{\pm} = \left| - \frac{1}{2} A_{\perp} - \nu_F \pm \frac{1}{8\nu_M} ({}^1A_{\parallel}^2 + {}^1A_{\perp}^2) \right|$$

$$\nu_F = g_N^F \beta_N |B| . \tag{13}$$

Introducing the measured constants ${}^1A_{\parallel}$ and ${}_1A_{\perp}$ together with the experimental parameters ν_M, B into (13) one calculates a secondary splitting of 81 kHz for $\vec{B} \parallel (y, z)$. The measured splitting is 87 ± 9 kHz (Fig. 14). Some splitting exists of course for any direction of $\vec{B}$ but due to the considerable line width for all other directions of $\vec{B}$ it is only resolved when $B \parallel (y, z)$. The large line width is to a great deal due to mosaic effects. It is in fact evident from Table VI that with decreasing anisotropy of the shfs tensor the line width decreases.

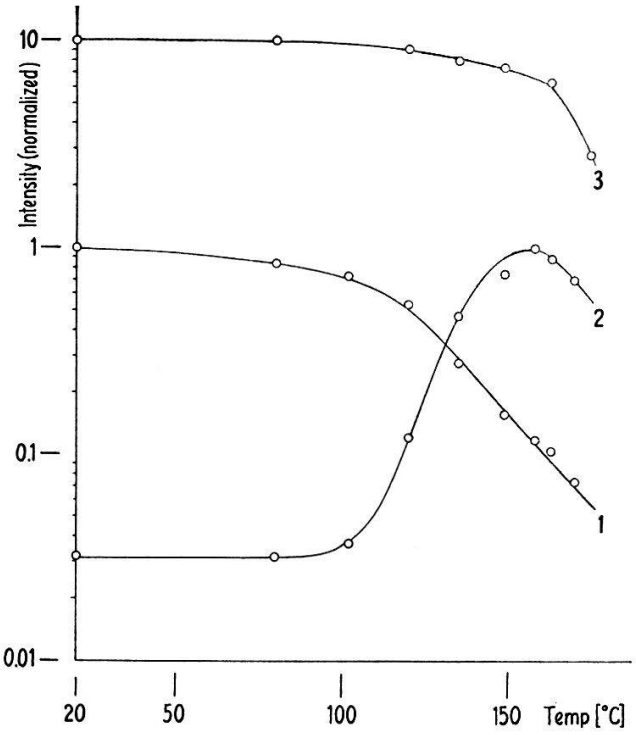

Figure 14

Annealing plot showing the thermal stability of the two centres simultaneously present in CaF_2. Curve 1 represents the intensity of the EPR spectrum of the centre involving one oxygen ion in arbitrary units as a function of the annealing temperature. Curve 2 furnishes the analogue information for (YO_2). Curve 3 shows the intensity of the optical absorption of the transition at 571 mμ of the Y^{2+}_{cubic} ion. For sake of clarity this curve is shifted upwards in the plot by a factor of 10. The plot exhibits the transfer of holes from the centre involving one oxygen ion to the (YO_2) centre between 100 and 150 °C. (The three curves are suitably normalized.)

---

[1]) Only nuclei 2, 3, 4, 5 are considered. Neglecting bending of the wave function ($\delta_0 = 0$, $\beta = 0$) the four nuclei have $D_{\infty h}$ symmetry. $\vec{B}$ situated in (y, z) reduces this symmetry to C_{2V}. Classification of $|{}^4I> \times |{}^5I>$ according to C_{2V} yields matrices 3×3 and 1×1.

Table VI

Width of the ENDOR lines of different sets of nuclei (see Figure 10)

Lable of the set	Direction of $\vec{B}$	Line width in kHz
4, 5	$\vec{B} \parallel x$	280
	$\vec{B} \parallel [1, 1, 1]$	320
	$\vec{B} \parallel (y, z)$	32
1		10
8	$\vec{B} \parallel x_2$	40
10	$\vec{B} \parallel x_2$	40
6	$\vec{B} \parallel x_1$	35

Cinetics of the Centres

All the experiments reported in this section have been performed on samples containing about equal concentration of sites where Y^{3+} ions have two or one or no oxygen ions located in their direct neighbourhood.

For briefness the centre involving one oxygen ion is designed by P centre in this section.

Firstly the formation of the centres as a function of irradiation time (t_T) has been investigated. X raying at room temperature yields the following two reactions in the purest investigated CaF_2 crystals (purest with respect to unwanted impurities).

$$0 \leqslant t_T \leqslant 1/2 - 1\,h \quad Y^{3+}_{\text{cubic}} + P^- + (YO_2)^- + h\nu \rightarrow Y^{2+}_{\text{cubic}} + P^0 + (YO_2)^- \qquad \text{(a)}$$

$$1/2 - 1\,h < t_T \qquad Y^{2+}_{\text{cubic}} + P^0 + (YO_2)^- + h\nu \rightarrow Y^{2+}_{\text{cubic}} + P^- + (YO_2)^0\,. \qquad \text{(b)}$$

In the first reaction the P^- complexes form together with the Y^{3+} ions in cubic symmetry (written Y^{3+}_{cubic} ion) an electron donor-acceptor system (the Y^{2+} ion with neighbouring interstitial F^- charge compensation is not stable at room temperature). The role of the $(YO_2)^-$ is insignificant here due to the relatively low ionisation probability.

As soon as most of the P^- complexes are ionized the $(YO_2)^-$ become the dominant electron donors. But the electron acceptors have trapped an electron. They are thus already converted to Y^{2+}_{cubic} ions which involve no excedent local charge with respect to the bulk of the crystal lattice. They are thermally very stable. GOERLICH et al. [21] have shown by thermoluminescence measurements that the lower limit of intrinsic thermal stability of the Y^{2+}_{cubic} ions in CaF_2 is situated between 300 and 400 °C. Let us remark by the way that in SrF_2 the Y^{2+}_{cubic} ion is instable already at room temperature.

The P centres instead involve one excedent positive charge unit with respect to the lattice. They thus act as electron acceptors as described by reaction (b) being converted to the nonmagnetic state P^-.

Annealing experiments have been performed on samples previously x rayed for 1/2 h at room temperature. The initial charge state of the centres is thus described by the right side of reaction (a).

In Figure 14 are depicted the results of a typical thermal annealing run. The concentration of the P centres and of the (YO_2) was measured by EPR and the concentration of the Y^{2+}_{cubic} ions was obtained from their four optical absorption bands (at 571, 396, 332, 226 mμ in CaF_2). The graph exhibits the transfert of holes from the thermally less stable P centres to the still unionized (YO_2^-) complexes which involve one negative charge unit with respect to the bulk of the lattice. The Y^{2+}_{cubic} ions are unaffected by this charge transfert. Their concentration begins only to decrease when the (YO_2) centres decay by releasing a hole.

The hole transfert between the P centre and the $(YO_2)^-$ has also been observed in SrF_2 crystals. However the stable electron traps are in this case not furnished by Y^{2+}_{cubic} (as they are not stable), but by REions introduced for this purpose into the crystals.

Correlation between the EPR spectrum of the (YO_2) centre and an optical absorption band (at 486 mμ in CaF_2 and 510 mμ in SrF_2) attributed to this centre has further been established by annealing experiments. Figure 15 shows the results obtained with SrF_2 samples. In this crystal the optical absorption is not masked by the four absorption bands of the Y^{2+}_{cubic} ions as in the CaF_2 crystals. The hole transfert from the P centre (the corresponding curve is not shown) to the $(YO_2)^-$ explains the enhancement of the EPR intensity of the latter. The important fact is that the intensity of the optical absorption and of the corresponding EPR signal grow together. Furthermore the whole annealing curves are the same. The same over all features of the EPR and optical absorption intensity are also observed in CaF_2 crystals. It is thus concluded that the observed optical transition is due to the (YO_2) centre. However, one simple alternative explication cannot be ruled out although it is unlikely. The

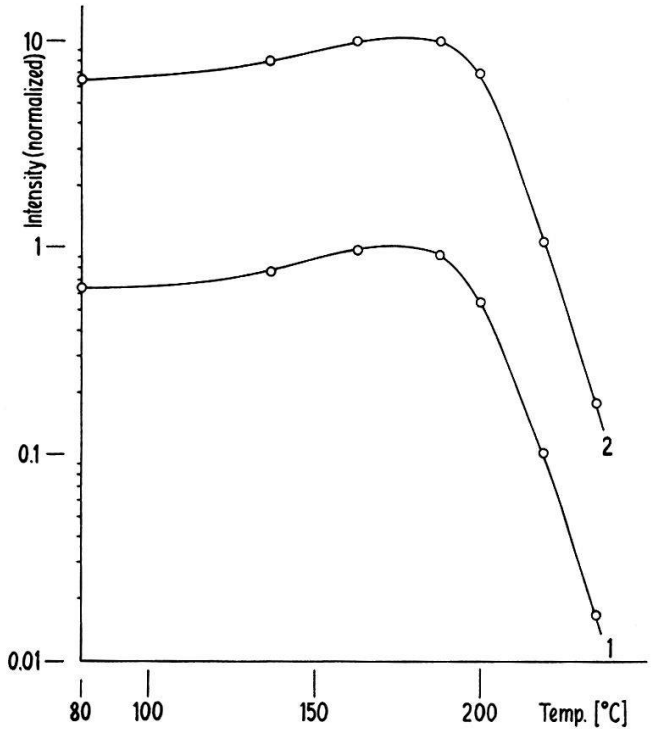

Figure 15

Annealing plot of the (YO_2) centre in SrF_2. The plot exhibits that the intensity of the optical absorption at 510 mμ attributed to this centre (1) and the intensity of the EPR spectrum (2) give congruent curves both being suitably normalized.

optical absorption might arise from a hole centre which shows the same thermal annealing characteristics as the (YO_2) but which exhibits no EPR spectrum at liquid He temperature and above in both charge states it can take.

Acknowledgement

The author would like to thank Prof. Dr. R. LACROIX (Directeur de thèse) for his interest, valuable advice and repeated discussions and to Prof. Dr. W. KÄNZIG (ETH, Zürich) for his interest, discussions and valuable critical comments.

Some discussions with Pd. Dr. K. A. MÜLLER (IBM, Rüschlikon) and Dr. J. SIERRO are acknowledged with thanks.

The author thanks also Mr. J. WEBER who did the necessary computer programming, to Mr. J. M. MORET for some drawings and occasional help in experiments and to Mr. D. v. MEYENBURG for his assistance in some of the experiments.

The financial support from the Swiss National Foundation for Scientific Research which made possible this investigation is gratefully acknowledged.

References

[1] W. BONTINCK, Physica *24*, 650 (1958).
[2] J. SIERRO, Helv. phys. Acta *36*, 505 (1963).
[3] W. KÄNZIG, Phys. Rev. *99*, 1890 (1955).
[4] T. G. CASTNER, W. KÄNZIG, J. Phys. Chem. Sol. *3*, 178 (1957).
[5] H. BILL, R. LACROIX, Phys. Lett. *21*, 257 (1966); J. de Phys. Suppl. *28*, C4–138 (1967).
[6] J. H. SCHULMAN, W. D. COMPTON, *Color Centers in Solids* (Pergamon Press 1962).
[7] J. R. O'CONNOR, J. H. CHEN, Phys. Rev. *130*, 1790 (1963).
[8] Purchased from YEDA, Israel.
[9] R. W. G. WYCKOFF, *Crystal Structures*, Vol. II (Interscience Publishers, New York).
[10] F. KNEUBÜHL, Phys. kondens. Mat. *1*, 410 (1965).
[11] B. BLEANEY, Phil. Mag. *42*, 441 (1951).
[12] V. HEINE, Phys. Rev. *107*, 1002 (1957).
[13] E. CLEMENTI, A. D. MCLEAN, Phys. Rev. *133*, A419 (1966).
[14] R. G. BARNES, W. V. SMITH, Phys. Rev. *93*, 95 (1954).
[15] G. HERZBERG, *Molecular Spectra*, Vol. II (D. Van Nostrand Comp., New York).
[16] A. M. CLOGSTON, J. P. GORDON, V. JACCARINO, M. PETER, L. R. WALKER, Phys. Rev. *117*, 1222 (1960).
[17] R. G. SHULMAN, S. SUGANO, Phys. Rev. *130*, 506 (1963).
[18] M. L. DAKS, R. L. MIEHER, Phys. Rev. Lett. *18*, No. 24, 1056 (1967).
[19] N. F. RAMSAY, E. M. PURCELL, Phys. Rev. *85*, 143 (1952).
[20] H. M. MCCONNELL, A. D. MCLEAN, C. A. REILLY, J. Chem. Phys. *23*, 1152 (1955).
[21] P. GOERLICH, H. KARRAS, A. KÖTHE, K. KÜHNE, Phys. stat. sol. *1*, 366 (1961).